Performance of a Hybrid Receiver in the Downlink Multicell CDMA System

Md Habibul Islam, Mohammad Saquib, *Member, IEEE*, and Naofal Al-Dhahir, *Senior Member, IEEE*

***Abstract*—In this paper, we propose a novel low-complexity receiver, namely, a hybrid receiver (HR) for the downlink of a multicell code-division multiple-access (CDMA) system with a transmit delay diversity transmission scheme. The proposed receiver is designed by combining the merits of the decorrelating receiver (DR) and the conventional receiver (CR). Unlike most multiuser receivers, HR operates with the same information as CR. For a target performance metric (e.g., bit error probability $(\mathrm{BEP}) = 10^{-2}$), the reduced-complexity HR significantly outperforms CR, DR, and minimum mean-square error (MMSE) receiver with estimated channel information. We also compare the performance of the reduced-complexity HR with a reduced-complexity MMSE receiver, which slightly outperforms the former at a price of higher complexity.**

***Index Terms*—Code-division multiple-access (CDMA) system, conventional receiver (CR), decorrelating receiver (DR), eigenvalue decomposition, intercell interference, intracell interference, minimum mean-square error (MMSE) receiver, multicell, signal-to-interference-plus-noise ratio (SINR).**

I. Introduction

CODE-DIVISION multiple-access (CDMA) systems have been commercially deployed to support multimedia traffic in mobile radio systems. Voice-based CDMA systems (e.g., IS-95) are generally symmetric in their uplink and downlink traffic, whereas in third generation (and beyond) CDMA systems, which support data traffic together with voice messages, the downlink carries the major portion of the total system traffic. In practical CDMA systems, such as IS-95 and CDMA2000, under ideal conditions (no multipath), the downlink is free from intracell interference due to the use of orthogonal Walsh codes. However, in practice, the orthogonality of the codes is destroyed when the downlink intracell signals are received by a user through a multipath channel. In next-generation CDMA systems, where multiple antennas will be used with sufficient spacings between them, it will not be possible to guarantee good cross-correlation properties among the downlink intracell received signals. Thus, designing effective low-complexity interference suppression schemes for the downlink CDMA system is an important area of research.

The idea of equalizing the downlink channel to restore orthogonality among the users' spreading sequences and thus reduce the interference has been proposed in numerous works (c. f. [1]–[4]). Two types of channel equalization have been considered in these works: zero-forcing and minimum mean-square error (MMSE). Zero-forcing equalization completely eliminates the multiple-access intracell interference introduced by multipath. However, it enhances the noise variance and intercell interference. Finite-impulse-response (FIR) linear MMSE equalization, which is computationally very complex, is used to minimize the noise enhancement associated with the zero-forcing equalization and to suppress the intercell interference. In [1], an average MMSE chip equalizer and its symbol-level adaptive version is proposed to reduce the complexity of linear MMSE chip equalizers. All these prior works on downlink channel equalization considered a single-antenna element at the base station.

Multiple-antenna open-loop transmit diversity schemes do not require downlink channel knowledge at the transmitter and, therefore, are very attractive for scenarios where channel estimation and tracking is difficult. Some open-loop transmit diversity schemes without using extra resources, (e.g., extra spreading codes for the downlink CDMA) include orthogonal transmit diversity (OTD) [5], space–time transmit diversity [6], space–time spreading (STS) [7], transmit delay diversity (TDD) [8], and multiphase spreading (MPS) [9]. The works of [5] and [7] put more emphasis on diversity than on multiple access interference (MAI). Although the decorrelating detector in [9] can mitigate the MAI, it requires knowledge of the other users' codes. In [10], the Rake receiver and the MMSE receiver are developed for OTD, STTD, and STS schemes, and using the derived SNR expressions, the performance of these three schemes are compared for both receivers. Reference [11] discusses the relative performance of OTD, STS, and TDD using both Rake and signal-to-interference-plus-noise ratio (SINR) maximizing (max-SINR) receivers. It shows that in the noiseless case, the zero-forcing equalizer is the max-SINR receiver under the TDD scheme. The filtering operation under the decorrelating receiver (DR) is the same as that of a zero-forcing equalizer, which eliminates the intracell multiuser interference by employing the pseudoinverse of the channel matrix on the received signal vector followed by despreading. We prove that in the downlink of a single-cell CDMA system, the performance of DR is the same as the conventional decorrelating receiver [12,

Manuscript received February 22, 2005; revised April 1, 2006. The associate editor coordinating the review of this manuscript and approving it for publication was Prof. Javier Garcia-Frias.

M. H. Islam was with the Wireless Communications Research Laboratory (WiCoRe), the University of Texas at Dallas, Richardson, TX 75083-0688 USA. He is now with the Department of Embedded Systems, Institute for Infocom Research (I2R), Singapore 119613, Singapore (e-mail: habibul@i2r.a-star.edu.sg).

M. Saquib is with Wireless Communications Research Laboratory (WiCoRe), The University of Texas at Dallas, Richardson, TX 75083-0688 USA (e-mail: saquib@utdallas.edu).

N. Al-Dhahir is with BITS, University of Texas at Dallas, Richardson, TX 75083-0688 USA (e-mail: aldhahir@utdallas.edu).

Color versions of one or more of the figures in this paper are available online at http://ieeexplore.ieee.org.

Digital Object Identifier 10.1109/TSP.2006.887106

Ch. 5] when all orthogonal codes are in use. The conventional decorrelating receiver [12] decodes the desired user's signal by zero-forcing the interfering users' signals with the knowledge of all active users' codes.

In this paper, we propose a novel low-complexity receiver for the downlink multicell CDMA system with TDD scheme, which we refer to as the *hybrid receiver* (HR). The proposed receiver HR efficiently combines the structures of conventional receiver (CR) and DR to provide a desirable tradeoff between the interference suffered by CR and the enhanced intercell interference and Gaussian noise suffered by DR. At the same time, HR preserves the key advantageous feature of CR and DR, namely that it operates without the knowledge of other users' codes. However, this would not be the case if we design linear multiuser receivers such as the decorrelating receivers of [13] and [14], the MMSE receiver of [15] and [16], and the partial decorrelating receiver of [17]. Moreover, the adaptive implementation of these receivers is not feasible when signature sequences of a user change from one symbol to another.

Since the main complexity in designing HR arises due to finding the eigenvectors of the channel autocorrelation matrix, we derive reduced-complexity HR (and DR) using the circulant approximation of the channel autocorrelation matrix [18] [in which the eigenvectors of the time-varying channel autocorrelation matrix are approximated by the time-invariant fast Fourier transform (FFT) basis vectors]. We also present a reduced-complexity MMSE receiver by approximating the eigenvectors of the average (over the coherence interval) received correlation matrix by the FFT basis vectors. Extensive Monte Carlo simulations are performed to compare the performance of HR and reduced-complexity HR with all other receivers of interest. We observe that for a target performance metric (e.g., bit error probability (BEP) $= 10^{-2}$), reduced-complexity HR provides significant capacity gains over the capacity of the average MMSE receiver, reduced-complexity DR, CR, and max-SINR receiver.

The remainder of this paper is organized as follows. In Section II, we describe the system and channel model. Section III presents the receiver designs; the analysis of the conditional BEP of DR; reduced-complexity implementations of HR, DR, and the average MMSE receiver; and the complexity analysis. Simulation results are given in Section IV, and the paper is concluded in Section V. In this paper, we use uppercase bold letters to denote matrices, lowercase bold letters to denote vectors, and uppercase or lowercase letters to denote scalars. We use notations $\mathbf{X}^\top$, $\mathbf{X}^\dagger$, and $\mathbf{X}^*$ to denote the transpose, Hermitian, and complex conjugate of matrix $\mathbf{X}$, respectively.

II. System Model

In a CDMA system, each symbol results in the baseband transmission of a sequence of pulses (or chips) of duration T_c seconds. The symbol duration is T seconds, and thus the processing gain is $N = T/T_c$. There are K users in the desired cell and without loss of generality, we assume that user 1 is the desired user and the transmitted symbols of user K are pilot symbols. Each base station transmits signals using two antennas, and each mobile in the system is equipped with a single antenna. The mth symbol of user q is $b_q(m)$. We consider the binary phase-shift keying (BPSK) signaling scheme[1] where information symbols of different users are equally likely ± 1 independent random variables. Thus, for $q \neq K$, $\mathbb{E}[b_q(m)] = 0$ and $|b_q(m)|^2 = 1$. However, the pilot symbol $b_K(m) = 1$. Let $\{s_q^{(j)}(m)\}_{j=1}^N$ be the complex chip sequences for symbol $b_q(m)$ at each antenna, where j is the chip index. The spreading sequence vector for symbol $b_q(m)$ at each antenna is $\mathbf{s}_q(m) = [s_q^{(1)}(m), \ldots, s_q^{(N)}(m)]^\top$. Sequences $\{s_q^{(j)}(m)\}$ and $\{s_k^{(j)}(m)\}$ are orthogonal for $q \neq k$ and they are normalized such that $\|\mathbf{s}_q(m)\|^2 = 1$. Similar to IS-95, these spreading sequences are derived by multiplying the orthogonal Walsh codes with the base-station-specific random codes. The total transmitter power for user q, denoted by P_q, is kept constant by splitting it equally among the two transmit antennas.

The transmitted signal of antenna g arrives at user 1 over L paths and the delay caused by path l is $(l-1)T_c$. The base station applies the TDD transmission scheme by introducing a delay of $\tau_2 = LT_c$ at antenna 2. As a result, the multipath spread of the first user's channel is $\tau_{\max} = (2L-1)T_c$. User 1 processes the received signal for the mth symbol interval using an observation window of duration WT_c, where $W = N + 2L - 1$. We assume that the multipath spread $\tau_{\max}$ is much smaller than the symbol duration T, which allows us to ignore intersymbol interference. If this is not the case, we will employ a symmetric (over the desired symbol) observation window of several symbols duration.

At the end of the mth symbol interval, the chip matched filter outputs yield the contribution from user q to the received signal of user 1 as

$$\mathbf{y}_q(m) = b_q(m)\sqrt{P_q}\mathbf{H}\mathbf{s}_q(m) \tag{1}$$

where $\mathbf{H}$ is an $W \times N$ matrix whose components are the functions of parameters of two downlink multipath channels and the structure of the transmitter pulse $p[t]$. If the contribution of antenna g to $\mathbf{H}$ is $\mathbf{H}_g$, then under the TDD scheme, $\mathbf{H}$ is expressed as $\mathbf{H} = (1/\sqrt{2})\sum_{g=1}^2 \mathbf{H}_g$, where the factor $1/\sqrt{2}$ is due to splitting the total transmitter power equally among two transmitting antennas. The size of $\mathbf{H}_g$ is the same as that of $\mathbf{H}$. To describe the channel matrix $\mathbf{H}_g$, we denote $h_g^{(l)}$ as the complex fade of path l of antenna g and write $\mathbf{h}_g^{(j)} = [\mathbf{0}(p_g^{(j)}), \tilde{\mathbf{h}}_g, \mathbf{0}(W - L - p_g^{(j)})]^\top$, where $j = 1, \ldots, N$, $p_g^{(j)} = j - 1 + (g-1)L$ and $\tilde{\mathbf{h}}_g = [h_g^{(1)}, \ldots, h_g^{(L)}]$. The notation $\mathbf{0}(l)$ denotes the all-zero row vector of size l. Combining the expressions for $\mathbf{H}$ and $\mathbf{h}_g^{(j)}$, we write the contribution of antenna g to the channel matrix $\mathbf{H}$ as $\mathbf{H}_g = [\mathbf{h}_g^{(1)}, \ldots, \mathbf{h}_g^{(N)}]$. Notice that we have omitted the subscript 1 from $\mathbf{H}$ because in the downlink all intracell users' signals come through the same channel of the desired user.

[1]For simplicity, we restrict our analysis to BPSK signaling scheme. However, in simulations, we use both BPSK and quadrature phase-shift keying (QPSK) modulation schemes.

Lumping intercell interference into white Gaussian noise,[2] we finally write the overall signal received by user 1 as

$$\mathbf{y}(m) = \mathbf{H}\sum_{q=1}^{K} b_q(m)\sqrt{P_q}\mathbf{s}_q(m) + \mathbf{n}(m) \tag{2}$$

where $\mathbf{n}(m)$ is a complex white Gaussian noise with covariance matrix $\sigma^2\mathbf{I}_W$, where $\mathbf{I}_W$ is an identity matrix of size $W \times W$.

III. Receiver Design

The three receiver structures of interest, namely DR, CR, and HR, consist of a maximum ratio combiner (MRC) at the front ends followed by their own filters. MRC applies linear transformation $\mathbf{H}^\dagger$ on the chip matched-filter output vector $\mathbf{y}(m)$ in (2) yielding in the output of MRC as

$$\tilde{\mathbf{y}}(m) = \mathbf{H}^\dagger\mathbf{H}\sum_{q=1}^{K} b_q(m)\sqrt{P_q}\mathbf{s}_q(m) + \mathbf{H}^\dagger\mathbf{n}(m) \tag{3}$$

where $\mathbf{H}^\dagger\mathbf{n}(m)$ is a zero-mean Gaussian $N\times 1$ noise vector with covariance matrix $\mathbb{E}[\mathbf{H}^\dagger\mathbf{n}\mathbf{n}^\dagger\mathbf{H}] = \sigma^2\mathbf{H}^\dagger\mathbf{H}$. The output of MRC is sent through the individual filter of each receiver which is presented in the following section. For simplicity, we will omit the symbol index (m) in the following development.

A. Conventional Receiver

Let $\mathbf{\Phi}_{\rm CR}$ denote the CR for symbol b_1, given by $\mathbf{\Phi}_{\rm CR} = \mathbf{s}_1$. Applying $\mathbf{\Phi}_{\rm CR}$ on the MRC output of (3), we find the decision statistic for symbol b_1 as

$$\begin{aligned} y_{\rm CR} &= \sqrt{P_1}b_1\mathbf{s}_1^\dagger\mathbf{H}^\dagger\mathbf{H}\mathbf{s}_1 + \sum_{q=2}^{K}\sqrt{P_q}b_q\mathbf{s}_1^\dagger\mathbf{H}^\dagger\mathbf{H}\mathbf{s}_q + \mathbf{s}_1^\dagger\mathbf{H}^\dagger\mathbf{n} \\ &= y_{\rm CR}^{(\rm d)} + y_{\rm CR}^{(\rm i)} + n_{\rm CR} \end{aligned} \tag{4}$$

where $y_{\rm CR}^{(\rm d)}$, $y_{\rm CR}^{(\rm i)}$, and $n_{\rm CR}$ are the desired, intracell interference, and noise portions of the CR output, respectively, and derived explicitly.

Next, we derive $\Gamma_{\rm CR}$, the instantaneous SINR of symbol b_1 at the output of CR as a function of the eigenvalues and eigenvectors of the channel autocorrelation matrix $\mathbf{H}^\dagger\mathbf{H}$. The instantaneous SINR of symbol b_1 is defined as the ratio of the instantaneous received power of symbol b_1 to the sum of average (over the information symbols) interference and noise powers at the output of the receiver. Let $\mathbb{E}_{\rm CR}$, $I_{\rm CR}$, and $\sigma_{\rm CR}^2$ denote the instantaneous power of symbol b_1, average intracell interference, and noise powers, respectively, at the output of CR. Using the expressions of these terms derived in (23), (24), and (25) of the Appendix, respectively, the SINR of symbol b_1 at the output of CR is given by

$$\Gamma_{\rm CR} = \frac{P_1\left(\sum_{j=1}^{N}\lambda_j\left|\mathbf{s}_1^\dagger\mathbf{u}_j\right|^2\right)^2}{\sum_{q=2}^{K}P_q\left|\sum_{j=1}^{N}\lambda_j\mathbf{s}_1^\dagger\mathbf{u}_j\mathbf{u}_j^\dagger\mathbf{s}_q\right|^2 + \sigma^2\sum_{j=1}^{N}\lambda_j\left|\mathbf{s}_1^\dagger\mathbf{u}_j\right|^2} \tag{5}$$

where λ_j is the jth eigenvalue of $\mathbf{H}^\dagger\mathbf{H}$ and $\mathbf{u}_j$ is the corresponding eigenvector. In a multiple-access system, the main cause of the SINR degradation is the multiple-access interference (MAI), i.e., the first term in the denominator of (5). An increase in the number of in-cell users gives rise to MAI resulting in a decrease in $\Gamma_{\rm CR}$. Therefore, although CR is a good receiver choice for a single-user environment or for a lightly loaded system, it becomes highly suboptimum, even for a moderately loaded system.

In the next section, we describe DR which requires the same information as CR to decode a user's symbol. However, unlike CR, it completely eliminates intracell interference.

B. Decorrelating Receiver

Let $\mathbf{\Phi}_{\rm DR}$ be the DR for the desired symbol. It can be easily shown that the channel autocorrelation matrix $\mathbf{H}^\dagger\mathbf{H}$ at the output of MRC is a finite-order Hermitian Toeplitz matrix of order $2L$ with $h_0 = \sum_{g=1}^{2}\sum_{l=1}^{L}|h_g^{(l)}|^2 \geq 0$ in the main diagonal. Due to the Toeplitz structure of $\mathbf{H}^\dagger\mathbf{H}$, if h_j denotes the (j,m)th element of $\mathbf{H}^\dagger\mathbf{H}$ the (m,j)th element of $\mathbf{H}^\dagger\mathbf{H}$ would be h_j^*. It is trivial to show that $h_j = \sum_{k=j+1}^{L}(h_1^{(k-1)})^*h_1^{(k)} + (h_1^{(L)})^*h_2^{(1)} + \sum_{k=2}^{L}(h_2^{(k-1)})^*h_2^{(k)}$ for $j = 1,\ldots,L-1$, $h_j = \sum_{k=j-L+1}^{L}(h_1^{(k-j+L)})^*h_2^{(k)}$ for $j = L,\ldots,2L-1$, and $h_j = 0$ for $j > 2L$. Note that h_0 is the total temporal and spatial diversity offered by the system and h_j for $j = 1,\ldots,2L-1$ is contributed by the cross-correlation terms among the multipath fading coefficients. Using the finite-order Hermitian Toeplitz property of $\mathbf{H}^\dagger\mathbf{H}$ together with the fact that h_0 is a continuous random variable (thus, $h_0 \neq 0$ with probability 1), we can show that $\mathbf{H}^\dagger\mathbf{H}$ is always invertible, which is the necessary condition for the existence of DR. Now, we define the DR for the desired symbol as

$$\mathbf{\Phi}_{\rm DR} = (\mathbf{H}^\dagger\mathbf{H})^{-1}\mathbf{s}_1. \tag{6}$$

Under DR, the decision statistic for the desired symbol b_1 is obtained as

$$y_{\rm DR} = \sqrt{P_1}b_1 + \mathbf{s_1}^\dagger(\mathbf{H}^\dagger\mathbf{H})^{-1}\mathbf{H}^\dagger\mathbf{n} = y_{\rm DR}^{(\rm d)} + n_{\rm DR} \tag{7}$$

where $y_{\rm DR}^{(\rm d)}$ is the desired portion of $y_{\rm DR}$ derived explicitly and $n_{\rm DR}$ is a zero-mean complex Gaussian random variable with average power $\sigma_{\rm DR}^2 = \sigma^2\sum_{j=1}^{N}(1/\lambda_j)|\mathbf{u}_j^\dagger\mathbf{s_1}|^2$, which is obtained by applying the eigenvalue decomposition (EVD) of $(\mathbf{H}^\dagger\mathbf{H})^{-1}$.

Next, we state a theorem that will provide a valuable insight into the performance of DR.

[2]All three receivers of interest detect the desired symbol without knowledge of the intercell interference. Our analysis is based on the SINR of these receivers, which depends on the second moments of the interference and the Gaussian noise. Since the intercell interference and the Gaussian noise are mutually independent and both are independent of the desired user's signal, we lump them together. However, in our numerical study, we model the intercell interference explicitly.

Theorem 1: In the downlink of a single-cell CDMA system, irrespective of the number of orthogonal codes in use, the performance of DR is the same as the worst-case performance of the conventional decorrelating receiver [12].

The proof of Theorem 1 is given in the Appendix. Theorem 1 implies that if the number of active users in the downlink of a single-cell CDMA system is less than the processing gain, the conventional decorrelating receiver [12] outperforms DR. This result follows from the fact that DR detects the desired user's signal assuming all orthogonal codes are in use. However, this performance gain of the conventional decorrelating receiver is achieved at the cost of acquiring knowledge of all active intracell users' codes. In general, this information is not available to the users in the downlink. Moreover, in a CDMA system with long codes, the structure of the conventional decorrelating receiver changes from one symbol to another. Here, the adaptive implementation (references in [12, p. 271]) of the conventional decorrelating receiver is also not feasible.

Now, we derive the instantaneous SINR of symbol b_1 at the output of DR. Let $\mathbb{E}_{\rm DR}$ and $\sigma^2_{\rm DR}$ be the instantaneous power of symbol b_1 and the average noise power at the output of DR, respectively. Since $\sum_{j=1}^N |\mathbf{s}_1^\dagger \mathbf{u}_j|^2 = 1$, the instantaneous power of symbol b_1 at the output of DR can be written as $\mathbb{E}_{\rm DR} = P_1 = P_1(\sum_{j=1}^N |\mathbf{s}_1^\dagger \mathbf{u}_j|^2)^2$. Using $\mathbb{E}_{\rm DR}$ and $\sigma^2_{\rm DR}$, we obtain the instantaneous SINR of symbol b_1 at the output of DR as

$$\Gamma_{\rm DR} = \frac{\mathbb{E}_{\rm DR}}{\sigma^2_{\rm DR}} = \frac{P_1\left(\sum_{j=1}^N \left|\mathbf{s}_1^\dagger \mathbf{u}_j\right|^2\right)^2}{\sigma^2 \sum_{j=1}^N \frac{1}{\lambda_j}\left|\mathbf{u}_j^\dagger \mathbf{s}_1\right|^2}. \tag{8}$$

Comparing (5) with (8), we see that DR does not suffer from intracell interference. However, it experiences an enhancement, by a factor of $\sum_{j=1}^N |\mathbf{s}_1^\dagger \mathbf{u}_j|^2/\lambda_j$, in the average noise power. As long as the degrading effect of interference plus noise of CR is less severe than the degrading effect of the enhanced noise of DR, CR performs better than DR. This would be the case in a lightly loaded system. However, in a highly loaded system, the degrading effect of the enhanced noise of DR would be less severe than the degrading effect of interference plus noise of CR and hence the performance of DR would be superior. This fact motivates us to search for a receiver that suffers moderately from enhanced noise in a lightly loaded system and from interference in a highly loaded system under the constraint that this receiver should operate using the same set of information as required by DR and CR. As a first step, we analyze the conditional BEP of DR given $\mathbf{H}$ as well as the structures of DR and CR using the eigenvalues and eigenvectors of $\mathbf{H}^\dagger\mathbf{H}$. Then, we show how to efficiently combine the structures of DR and CR to design the proposed hybrid receiver, which is referred to henceforth as the HR.

C. Conditional Bit Error Probability Analysis

Given $\mathbf{H}$ and using the central limit theorem, $n_{\rm DR}$ can be approximated as a zero-mean complex Gaussian random variable with variance $\tilde{\sigma}^2_{\rm DR} = \sigma^2 \sum_{j=1}^N (1/\lambda_j)\mathbb{E}[|\ \mathbf{u}_j^\dagger \mathbf{s_1}\ |^2] = (\sigma^2/N)\sum_{j=1}^N (1/\lambda_j)$, where we used the result $\mathbb{E}[|\ \mathbf{u}_j^\dagger \mathbf{s_1}\ |^2] = \mathbf{u}_j^\dagger \mathbb{E}[\mathbf{s_1}\mathbf{s_1}^\dagger]\mathbf{u}_j = (1/N)$, which follows from the fact that spreading sequences are derived by multiplying the orthogonal Walsh codes with the base station's specific random codes. Therefore, the conditional BEP of symbol b_1 given $\mathbf{H}$ under DR is

$$P_{\rm b|\mathbf{H}} = Q\left[\sqrt{\frac{2P_1}{\tilde{\sigma}^2_{\rm DR}}}\right] = Q\left[\sqrt{\frac{2P_1}{(\sigma^2/N)\sum_{j=1}^N 1/\lambda_j}}\right] \tag{9}$$

where $Q[\cdot]$ represents the standard Q-function defined as $Q[x] = (1/2)\mathrm{erfc}(x/\sqrt{2})$.

From (9), it is clear that at the output of DR, the noise variance is increased by a factor of $(1/N)\sum_{j=1}^N 1/\lambda_j$. Since $1/\lambda_j$ is the eigenvalue of $(\mathbf{H}^\dagger\mathbf{H})^{-1}$, both the effect of channel decorrelation and the gain due to diversity are embedded in it. To see those effects explicitly, we decompose $\mathbf{H}^\dagger\mathbf{H}$ as a sum of two matrices as follows: $\mathbf{H}^\dagger\mathbf{H} = \mathbf{H}_{\rm D} + \mathbf{H}_\Delta$, where $\mathbf{H}_{\rm D}$ is an $N \times N$ diagonal matrix containing h_0 on the diagonal. The term $\mathbf{H}_\Delta$ is a Hermitian Toeplitz matrix whose diagonal elements are zero and off-diagonal elements are the same as those of $\mathbf{H}^\dagger\mathbf{H}$. Recall that h_0 is the total diversity offered by multipath and multiple antennas. Let the jth eigenvalue of $\mathbf{H}_\Delta$ be η_j, which satisfies $\lambda_j = h_0 + \eta_j$ for $j = 1, \ldots, N$. Substituting λ_j into (9), we obtain the following expression for conditional BEP:

$$P_{\rm b|\mathbf{H}} = Q\left[\sqrt{\frac{2P_1}{(\sigma^2/N)\sum_{j=1}^N 1/(h_0+\eta_j)}}\right]. \tag{10}$$

Since the trace of $\mathbf{H}_\Delta$ is zero, we have $\sum_{j=1}^N \eta_j = 0$ [19], which implies that some of $\{\eta_j\}$ are non-negative and some of $\{\eta_j\}$ are negative. In (10), notice that when $\eta_j = 0$, $\lambda_j = h_0$ for all j and we achieve full diversity. Due to the monotonicity of the Q-function, the conditional BEP under DR will be higher for larger values of $(1/N)\sum_{j=1}^N (h_0 + \eta_j)^{-1}$. If $\eta_j < 0$, or $\lambda_j < h_0$, we lose some diversity resulting in increased BEP. Based on this analysis, we categorize the eigenvalues of $\mathbf{H}^\dagger\mathbf{H}$ into two groups, namely 1) "strong eigenvalues," where $\lambda_j \geq h_0$ and 2) "weak eigenvalues," where $\lambda_j < h_0$.

D. Hybrid Receiver

Now, we describe a novel receiver structure that compensates for the higher noise power caused by the 'weak eigenvalues' at the output of DR. Let us first look at the structures of both DR and CR. Using EVD of $\mathbf{H}^\dagger\mathbf{H}$, an alternate way to express DR and CR is

$$\mathbf{\Phi}_{\rm DR} = \sum_{j=1}^N \frac{1}{\lambda_j}\mathbf{u}_j\mathbf{u}_j^\dagger \mathbf{s}_1; \quad \mathbf{\Phi}_{\rm CR} = \sum_{j=1}^N \mathbf{u}_j\mathbf{u}_j^\dagger \mathbf{s}_1. \tag{11}$$

Comparing the above expressions of $\mathbf{\Phi}_{\rm DR}$ and $\mathbf{\Phi}_{\rm CR}$, we observe that if we scale the eigenvalues of $\mathbf{H}^\dagger\mathbf{H}$ to 1, the filtering operation of DR will be the same as that of CR. Let the first M eigenvalues of $\mathbf{H}^\dagger\mathbf{H}$ be the "strong eigenvalues" and the rest $(N-M)$ be the "weak eigenvalues." Since the "weak eigenvalues" of $\mathbf{H}^\dagger\mathbf{H}$ are the ones that enhance the noise variance at the output of DR, the proposed HR uses the value of 1 in place of the actual value for the weak eigenvalues as it is the case in CR. Thus, the proposed HR is derived as

$$\mathbf{\Phi}_{\mathrm{HR}} = \sum_{j=1}^{M} \frac{1}{\lambda_j} \mathbf{u}_j \mathbf{u}_j^{\dagger} \mathbf{s}_1 + \sum_{j=M+1}^{N} \mathbf{u}_j \mathbf{u}_j^{\dagger} \mathbf{s}_1. \tag{12}$$

From (12), it is clear that HR is a hybrid version of DR and CR.

Applying $\mathbf{\Phi}_{\mathrm{HR}}$ on the MRC output, we find the decision statistic for b_1 under HR as

$$y_{\mathrm{HR}} = y_{\mathrm{HR}}^{(\mathrm{d})} + y_{\mathrm{HR}}^{(\mathrm{i})} + n_{\mathrm{HR}} \tag{13}$$

where $y_{\mathrm{HR}}^{(\mathrm{d})}$, $y_{\mathrm{HR}}^{(\mathrm{i})}$, and n_{HR} are the desired, intracell interference, and noise terms, respectively, at the output of HR. The expressions for $y_{\mathrm{HR}}^{(\mathrm{d})}$ are $y_{\mathrm{HR}}^{(\mathrm{i})}$ are derived in (26) and (27) of the Appendix, respectively. The noise term n_{HR} at the output of HR and can be expressed as

$$n_{\mathrm{HR}} = \left(\sum_{j=1}^{M} \frac{1}{\lambda_j} \mathbf{s}_1^{\dagger} \mathbf{u}_j \mathbf{u}_j^{\dagger} + \sum_{j=M+1}^{N} \mathbf{s}_1^{\dagger} \mathbf{u}_j \mathbf{u}_j^{\dagger} \right) \mathbf{H}^{\dagger} \mathbf{n}. \tag{14}$$

If Γ_{HR}, $\mathbb{E}_{\mathrm{HR}}$, I_{HR}, and σ_{HR}^2 denote the instantaneous SINR, instantaneous power of symbol b_1, average power of intracell interference, and noise at the output of HR, respectively, then $\Gamma_{\mathrm{HR}} = \mathbb{E}_{\mathrm{HR}}/(I_{\mathrm{HR}} + \sigma_{\mathrm{HR}}^2)$. The expressions for $\mathbb{E}_{\mathrm{HR}}$, I_{HR} and σ_{HR}^2 are derived in (28), (29), and (30) of Appendix, respectively. Comparing the expression for Γ_{HR} with (5) and (8), we can see, as expected, that the instantaneous SINR equation of HR is also a combination of that of CR and DR. When most of the eigenvalues of $\mathbf{H}^{\dagger}\mathbf{H}$ are strong, i.e., $M = N$, HR operates like DR and $\Gamma_{\mathrm{HR}} = \Gamma_{\mathrm{DR}}$. On the other hand, if most of the eigenvalues of $\mathbf{H}^{\dagger}\mathbf{H}$ are weak, HR operates like CR in which case Γ_{HR} looks more like Γ_{CR}. These are the two extreme cases of the performance of HR. Thus, when some of the eigenvalues are strong and some are weak, HR is a hybrid version of DR and CR.

E. MMSE Receivers

Next, to compare the performance of the proposed HR, we present the expressions for two MMSE receivers, namely the average MMSE receiver [1] and max-SINR receiver [11] using our system model. The performance of these receivers are of interest since they are designed to minimize the noise enhancement associated with zero-forcing equalization and also to suppress intracell and intercell interference. Let $\mathbf{\Phi}_{\mathrm{MMSE}}$ and $\mathbf{\Phi}_{\mathrm{MAXSINR}}$ denote the average MMSE receiver and max-SINR receiver, respectively. According to the definition of [1], the average MMSE receiver is given by

$$\mathbf{\Phi}_{\mathrm{MMSE}} = \frac{P_1}{N} \left(\frac{1}{N} \sum_{q=1}^{K} P_q \mathbf{H}\mathbf{H}^{\dagger} + \sigma^2 \mathbf{I}_W \right)^{-1} \mathbf{H}\mathbf{s}_1. \tag{15}$$

Using the average received correlation matrix $\bar{\mathbf{R}} = (1/N) \sum_{q=1}^{K} P_q \mathbf{H}\mathbf{H}^{\dagger} + \sigma^2 \mathbf{I}_W$, the max-SINR receiver derived according to [11] is given by

$$\mathbf{\Phi}_{\mathrm{MAXSINR}} = \bar{\mathbf{R}}^{-1} \mathbf{H} (\mathbf{H}^{\dagger} \bar{\mathbf{R}}^{-1} \mathbf{H})^{-1} \mathbf{s}_1. \tag{16}$$

F. Reduced-Complexity Receivers

Although both HR and DR use the same set of information as CR to decode the desired user's signal, the practical implementations of HR and DR are dominated by the high complexities of finding the eigenvectors and eigenvalues of $\mathbf{H}^{\dagger}\mathbf{H}$ for HR and inverting $\mathbf{H}^{\dagger}\mathbf{H}$ for DR. Since these receivers are implemented in the downlink, battery power at the mobile becomes a limiting factor to perform these operations. We propose low complexity implementations of HR and DR by approximating the eigenvectors of $\mathbf{H}^{\dagger}\mathbf{H}$ by the FFT basis vectors.

In [18], it is shown that any finite-order Toeplitz matrix of size $n \times n$ and order $m + 1$ can be approximated by a circulant matrix if $n \gg m$. Since $\mathbf{H}^{\dagger}\mathbf{H}$ is an $N \times N$ finite-order Toeplitz matrix of order $2L$ and in practice $N \gg 2L$, the circulant approximation allows us to approximate the eigenvectors of the time-varying channel autocorrelation matrix $\mathbf{H}^{\dagger}\mathbf{H}$ by the columns of the time-invariant FFT matrix $\mathbf{F}$ defined as

$$\mathbf{F} = \sqrt{N}\{e^{i2\pi mk/N}; m, k = 0, 1, \ldots, N-1\} \tag{17}$$

where $i = \sqrt{-1}$ is a complex number. Using $\mathbf{F}$, the jth eigenvalue of $\mathbf{H}^{\dagger}\mathbf{H}$ is approximated as $\hat{\lambda}_j = (\mathbf{F}^{\dagger}\mathbf{H}^{\dagger}\mathbf{H}\mathbf{F})_{j,j}$, where $(\mathbf{A})_{j,j}$ denote the jth diagonal element of matrix $\mathbf{A}$. Using this approximation, we derive reduced-complexity DR and HR, respectively, as follows:

$$\hat{\mathbf{\Phi}}_{\mathrm{DR}} = \sum_{j=1}^{N} \frac{1}{\hat{\lambda}_j} \hat{\mathbf{u}}_j \hat{\mathbf{u}}_j^{\dagger} \mathbf{s}_1 \tag{18}$$

$$\hat{\mathbf{\Phi}}_{\mathrm{HR}} = \sum_{j=1}^{M} \frac{1}{\hat{\lambda}_j} \hat{\mathbf{u}}_j \hat{\mathbf{u}}_j^{\dagger} \mathbf{s}_1 + \sum_{j=M+1}^{N} \hat{\mathbf{u}}_j \hat{\mathbf{u}}_j^{\dagger} \mathbf{s}_1 \tag{19}$$

where $\{\hat{\lambda}_j\}_{j=1}^{N}$ are the approximated eigenvalues of $\mathbf{H}^{\dagger}\mathbf{H}$ in descending order and $\{\hat{\mathbf{u}}_j\}_{j=1}^{N}$ are the corresponding approximated eigenvectors which are the columns of $\mathbf{F}$.

Now, to compare the performance of the reduced-complexity HR and DR, we introduce the low-complexity implementation of the average MMSE receiver [1]. From (15), we see that the average MMSE receiver can be directly calculated from knowledge of the average received correlation matrix $\bar{\mathbf{R}}$ which is, in turn, obtained from knowledge of the channel matrix, the sum powers received from the desired base station, and the noise covariance matrix which includes intercell interference. However, in practice, $\bar{\mathbf{R}}$ needs to be estimated. One way to estimate $\bar{\mathbf{R}}$ is to take the time-average of $\mathbf{R} = \mathbf{y}(m)\mathbf{y}^{\dagger}(m)$. Since $\mathbf{R}$ is a rank-one matrix, it is ill-conditioned, and good estimation of $\bar{\mathbf{R}}$ requires averaging over many symbols within the coherence interval which is not possible in a rapidly time-varying channel. The poor estimation of $\bar{\mathbf{R}}$ negatively affects the performance of the average MMSE receiver.

It should be noted that $\bar{\mathbf{R}}$ with perfect knowledge of the channel matrix, the sum powers of the serving base station, and noise covariance matrix is a nearly Toeplitz matrix in the sense that most of its diagonal elements are equal except $2L - 1$ elements at both ends of the diagonal. Moreover, $\bar{\mathbf{R}}$ is a sparse matrix, whereas the estimated $\bar{\mathbf{R}}$ (which is denoted as $\hat{\mathbf{R}}$) would not be sparse due to the estimation effects of $\bar{\mathbf{R}}$ in a time-varying channel. Since the order of $\bar{\mathbf{R}}$ depends not only on the mulitpath delay profile of the desired base station but also on that of other interfering base stations, it would be difficult to modify the structure of $\bar{\mathbf{R}}$ to be a sparse Toeplitz matrix. We present reduced-complexity MMSE receiver by approximating the eigenvectors of $\hat{\mathbf{R}}$ by the FFT basis vectors. This approximation serves two purposes: 1) it reduces the complexity of inverting $\bar{\mathbf{R}}$ and 2) it modifies the structure of $\hat{\mathbf{R}}$ towards a circulant matrix (which is a sparse Toeplitz matrix). We will see later that the above modification of the structure of $\hat{\mathbf{R}}$ dramatically improves the performance of the estimated average MMSE receiver.

Now, we describe the process of deriving reduced-complexity MMSE receiver. First, we estimate the $W \times W$ average received correlation matrix as $\hat{\mathbf{R}} = (1/\beta)\sum_{n=1}^{\beta}\mathbf{y}(n)\mathbf{y}^{\dagger}(n)$, where β is the number of symbols within the coherence interval and $W = N + 2L - 1$ is the length of the observation window as defined in Section II. Let $\mathbf{F}_1$ be the $W \times W$ FFT matrix. To approximate the jth eigenvalue of $\hat{\mathbf{R}}$, we write $\hat{\gamma}_j = (\mathbf{F}_1^{\dagger}\hat{\mathbf{R}}\mathbf{F}_1)_{j,j}$. Using $\hat{\gamma}_j$, the reduced-complexity MMSE receiver is given by

$$\hat{\mathbf{\Phi}}_{\text{MMSE}} = \frac{P_1}{N}\sum_{j=1}^{W}\frac{1}{\hat{\gamma}_j}\hat{\mathbf{u}}_{1j}\hat{\mathbf{u}}_{1j}^{\dagger}\mathbf{H}\mathbf{s}_1 \tag{20}$$

where $\{\hat{\gamma}_j\}_{j=1}^{W}$ are the approximate eigenvalues of $\hat{\mathbf{R}}$ in descending order, and $\{\hat{\mathbf{u}}_{1j}\}_{j=1}^{W}$ are the corresponding approximated eigenvectors which are the columns of the FFT matrix $\mathbf{F}_1$.

G. Complexity Analysis

In this paper, our objective is to evaluate the performance of the receiver in terms of capacity as well as the complexity of implementing it. In this section, we quantify the computational complexity of CR and the proposed reduced-complexity receivers in terms of the number of multiplications required. Denoting $\mathcal{C}_{\text{CR}}$, $\mathcal{C}_{\text{HR}}$, and $\mathcal{C}_{\text{MMSE}}$ as the number of multiplications per coherence interval required to implement CR, reduced-complexity HR, and reduced-complexity MMSE receiver, respectively, we derive these quantities as[3] $\mathcal{C}_{\text{CR}} = NGL(\beta+1) + 2(GL+1)$, $\mathcal{C}_{\text{HR}} = NGL(\beta+1) + (1/2)(GL+1)(GL+4) + N(GL-1)(3GL-2) + N(2GL-1)(N-2GL+2) + 3N^2 + 2(M-N)$, and $\mathcal{C}_{\text{MMSE}} = W^3 + W^2(\beta+4) + W(NGL+3) + NGL(\beta+N+2) + GL(\beta N+2) + 5$. In the above expressions, G is the number of transmitting antennas, therefore, $W = N + GL - 1$, N and L are as defined in Section II, and M is the number of strong eigenvalues. Comparing, $\mathcal{C}_{\text{CR}}$, $\mathcal{C}_{\text{DR}}$, and $\mathcal{C}_{\text{HR}}$, we can easily see that the complexities of CR, reduced-complexity HR, and reduced-complexity MMSE receiver are $\text{O}(\beta NGL)$, $\text{O}(2N^2GL)$, and $\text{O}(W^3)$, respectively. To make the complexity comparison more apparent, we quantify it using some typical values for the parameters. Let $N = 64$, $G = 2$, $L = 2$, and $M = N = 64$. Note that $M = N$ is the worst-case complexity of reduced-complexity HR, because in this case, in $\mathcal{C}_{\text{HR}}$ the term $2(M-N)$ has the highest number of multiplications. Let $\beta = 32$, which corresponds to 45-mi/h vehicle speed for 2GHz carrier frequency. For the above parameters, the number of multiplications required for CR, reduced-complexity HR and reduced-complexity MMSE receiver are 8458, 48660, and 487925, respectively. Hence, the complexity of reduced-complexity HR is at most 5.8 times that of CR, whereas the complexity of reduced-complexity MMSE receiver is at least ten times that of reduced-complexity HR. We use the word at least because in case $M < N$, the number of multiplications to calculate reduced-complexity HR would be less than 48 660. Moreover, from the expressions of $\mathcal{C}_{\text{CR}}$, $\mathcal{C}_{\text{DR}}$, and $\mathcal{C}_{\text{HR}}$, it is straightforward to see that with the increase in coherence interval and processing gain, the increase in the complexity of reduced-complexity MMSE receiver will be more than the increase in the complexity of both CR and reduced-complexity HR.

[3]Multipath channel coefficients are estimated using a matched filter receiver. Most of the multiplications are complex in nature. The inversion of a number is equivalent to one multiplication.

IV. Simulation Results

For our simulations, we model a multicell CDMA system with seven equally loaded contiguous circular cells. The center cell is assumed to be the desired cell. The radius of each cell is $r_{\text{d}} = 2000$ meters and mobiles are uniformly distributed within the desired cell. This assumption yields a probability density function $f(r) = 2r/r_{\text{d}}^2$ for the distance of a user from the desired base station. The path loss exponent is 4. The height of the base station is 30 m so that the downlink channel gain to a user from the base station is $h = 1/(r_{\text{d}}^2 + 30^2)^2$. The number of transmitting antennas at the base station is two. The channel attenuation coefficient of each path is modeled as an independent identically distributed complex zero-mean Gaussian random variable with average power $1/2L$. The length of the spreading sequences is 64. Similar to IS-95, these spreading sequences are derived by multiplying the orthogonal Walsh codes with the base-station-specific random codes. The background noise variance $\sigma^2 = 1$. Each base station uses the same transmitter power for all its users.[4] The transmitter powers of all seven base stations are also the same. Thus, the received signal-to-noise ratio (SNR) at each cell boundary is the same for all users. In most experiments, we plot BEP against the load per cell defined as $K \times d/L$, where d is the dimension of the modulation schemes (e.g., $d = 1$ for BPSK and $d = 2$ for QPSK modulation schemes). We use BPSK modulation scheme except in the last experiment where we use gray-coded QPSK modulation scheme. We use the abbreviations "Perf.," "Est.," "Approx.", and "c." to denote perfect channel state information (CSI), estimated CSI, reduced-complexity implementation of receivers, and simulation with coding, respectively.

First, we investigate the hybrid characteristic of the proposed HR. In Fig. 1, we plot the average number of strong eigenvalues normalized by the processing gain (i.e., $\mathbb{E}[M]/N$) as a function of the number of paths per transmitting antenna. Here, we use the perfect CSI. Notice that for $L = 1$, $\mathbb{E}[M]/N \approx 0.5$ and as the number of paths per transmitting antenna increases, the average number of strong eigenvalues decreases. This result suggests that as the number of paths per transmitting antenna increases, HR starts to operate more like CR than DR.

[4]The real systems like CDMA2000 and WCDMA utilize power control and therefore the results presented here are not directly applicable to those systems.

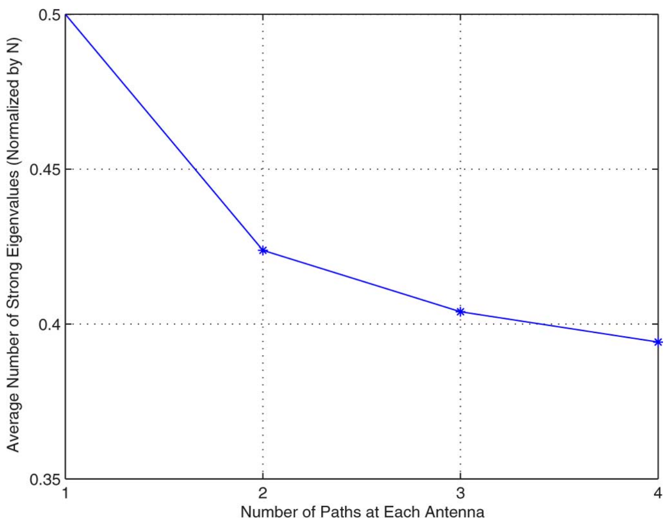

Fig. 1. Average number of strong eigenvalues normalized by the processing gain (i.e., $\mathbb{E}[M]/N$) as a function of the number of paths per transmitting antenna.

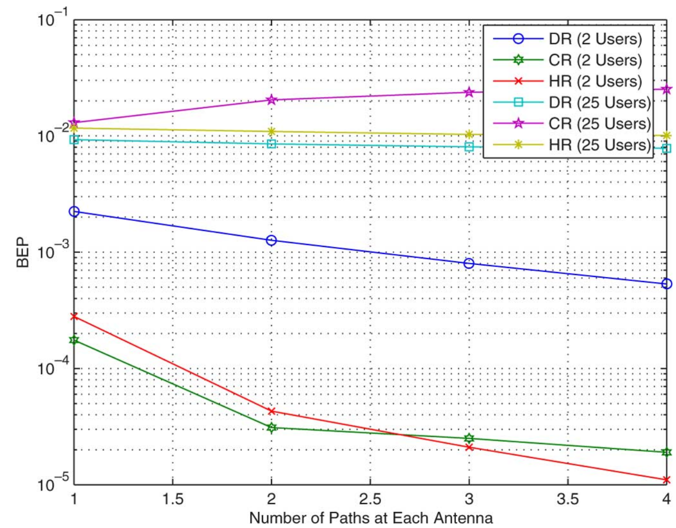

Fig. 3. Effect of the number of paths on the BEP. Here, the number of users per cell is two and SNR $= 12$ dB at each cell boundary and perfect CSI is assumed.

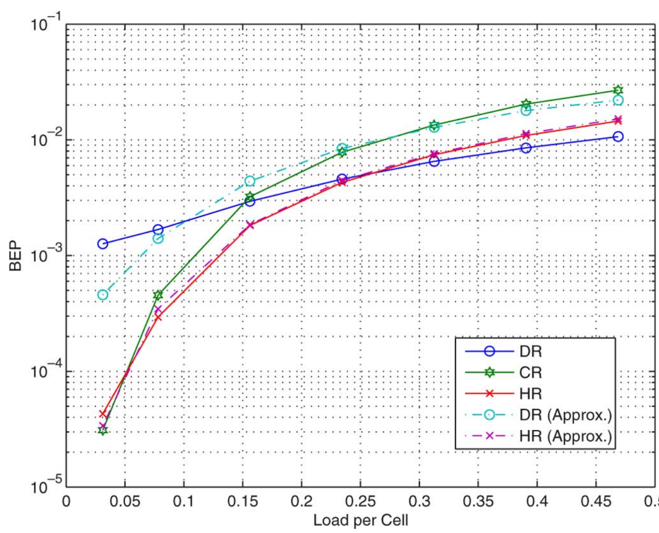

Fig. 2. Performance comparison of DR, CR and HR with reduced-complexity DR and HR using perfect CSI.

In our next experiment, we compare the performance of DR, CR and HR with that of reduced-complexity DR and HR assuming perfect CSI at the receiver. In Fig. 2, we plot the performance (BEP) of these receivers as a function of load per cell. Here SNR $= 12$ dB at each cell boundary and $L = 2$. Reduced-complexity DR and HR are denoted by DR (Approx.) and HR (Approx.), respectively. From Fig. 2, we observe that at a target BEP $= 10^{-2}$, DR (Approx.) suffers from a 38% decrease in capacity compared with DR, whereas the capacity of HR (Approx.) remains almost the same as the capacity of HR. This result suggests that HR is more robust to the errors caused by the circulant approximation of the channel autocorrelation matrix $\mathbf{H}^{\dagger}\mathbf{H}$. This observation is not surprising, because it is more difficult to approximate (or estimate) weak eigenvalues than to approximate (or estimate) strong eigenvalues and unlike HR, DR processes (or inverts) both weak and strong eigenvalues. It is also observed that for a lightly loaded system DR (Approx.) performs better than the DR. This result reflects the behavior of approximation, which does not yield an upper (or a lower) bound on the performance of DR.

Next, we investigate the effect of number of paths on the performance of DR, CR and HR assuming perfect CSI. In Fig. 3, we plot the BEP while varying the number of paths of each antenna. Here, the number of users per cell is 2 and 25, and SNR $= 12$ dB at the cell boundary. It is clear from Fig. 3 that in a lightly loaded system, all three receivers, especially CR and HR, gain in performance with the increase in the number of diversity branches. Note that although CR performs slightly better than HR for $L = 1$ and $L = 2$, HR starts to outperform CR as L increases to 3. In the case of 25 users, both DR and HR do not pick up significant performance gains from the increase in the number of paths. On the other hand, the performance of CR starts degrading as the number of paths increases. This result is explained as follows. Under CR, orthogonal Walsh codes completely eliminate the intracell interference when the number of transmitting antennas is one and $L = 1$. The gain from the orthogonality of the Walsh codes diminishes with the increase in the number of paths or transmitting antennas. When the system is highly loaded, the increase in the intracell interference (due to the increase in the number of paths) dominates over the diversity gain resulting from the increase in the number of paths for CR. On the other hand, for highly loaded systems, the performance of DR and HR remain almost constant as the number of paths increases.

Next, we investigate the performance of DR, CR, and HR as a function of SNR at each cell boundary in Fig. 4 assuming perfect CSI. In this experiment, $L = 2$, and the number of users at each cell is 15. At low SNR, HR outperforms CR and DR while CR outperforms DR. However, at 12 dB, the performance of DR becomes comparable to HR and at this point, both DR and HR outperform CR. At high SNRs (starting from 14 dB), DR performs better than both CR and HR. This result is expected because in our simulation an increase in the desired signal power causes a simultaneous increase in the interfering powers. Since, unlike

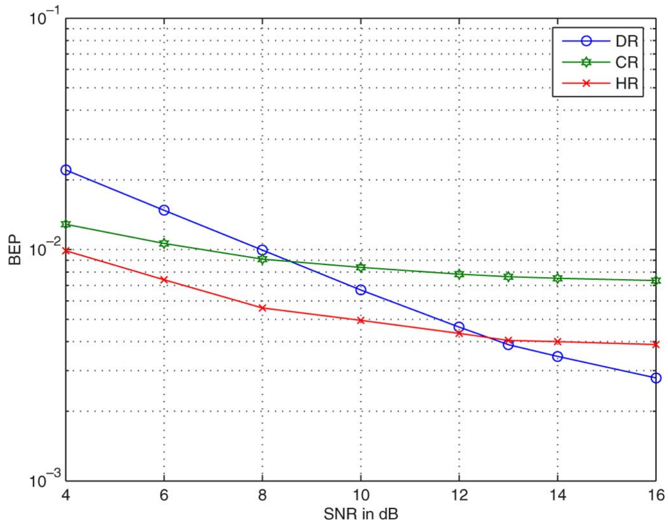

Fig. 4. BEP as a function of SNR at each cell boundary. Here, the number of users per cell is 15 and $L = 2$ and perfect CSI is assumed.

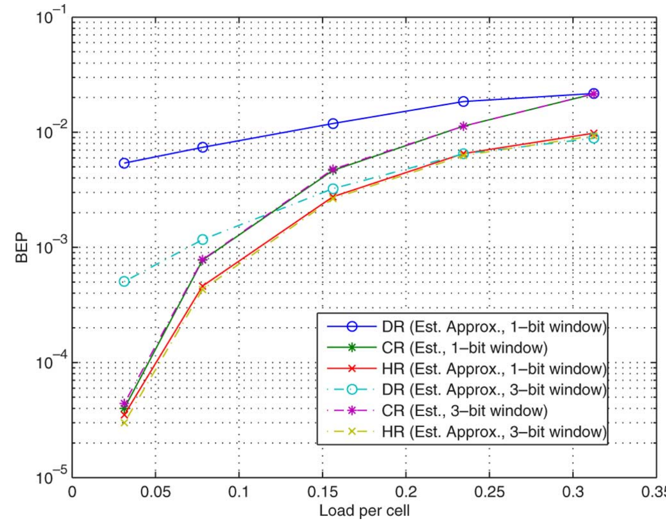

Fig. 6. BEP as a function of load per cell in ISI channel using estimated CSI. Here, SNR $=$ 12 dB per dimension.

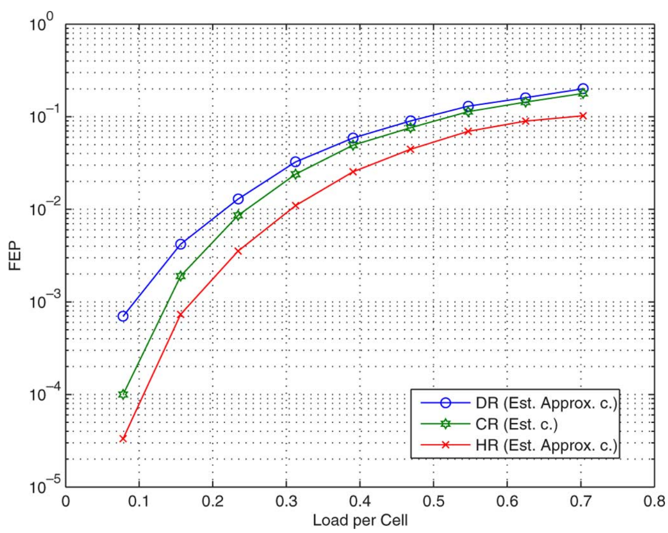

Fig. 5. FEP as a function of load per cell for eight fades within the frame using estimated CSI.

CR and HR, DR does not suffer from intracell interference, it realizes more performance gain from the increase in SNR. However, it should be noted that in a CDMA system with many cells, the transmitter power of a base station is controlled in order to avoid causing interference to other cells.

In the next experiment, we study in Fig. 5 the performance of reduced-complexity HR, reduced-complexity DR, and CR in terms of frame error probability (FEP) with respect to system load. Here, the receivers have estimated CSI. A 20-ms frame of a user consisting of 48 symbols is sent through a (2,1,9) convolutional encoder, which is used in the IS-95 standard. Bit interleaving is performed following the channel encoder, where channel encoded bits are written into the matrix along its columns and read out from its rows. In this experiment, $L = 2$, SNR $= 12$ dB at each cell boundary and the number of fades per path over one frame is eight, which corresponds to a 60-mi/h vehicle speed for a carrier frequency $f_c = 2$ GHz. The channel coefficients follows block-fading channel model and a soft Viterbi decoder is used. From Fig. 5, we see that for a target FEP $= 10^{-1}$, the reduced-complexity HR provides 30% capacity gain over CR.

In all the previous experiments, we ignore the effect of intersymbol interference (ISI) on the BEP performance. In this experiment, the performance of reduced-complexity HR, reduced-complexity DR and CR are compared in presence of ISI and each receiver operates with estimated CSI. Here, a frame of a user consists of 192 BPSK symbols and its duration is 20 ms. The coherence time of the channel is defined as $\Delta = (0.423/f_m)$ [20], where f_m is the maximum Doppler frequency. For velocity $v = 45$ mi/h and carrier frequency $f_c = 2$ GHz, the number of fades per path over one frame is approximately six. Each symbol gets interference from one previous symbol and one future symbol. The number of paths at each antenna is four. The desired frame is decoded by employing an observation window of both one-symbol and three-symbol duration. Fig. 6 shows that both CR and reduced-complexity HR shows similar performance irrespective of the length of the observation window. However, the performance of the reduced-complexity DR greatly degrades under one-symbol observation window. This result is explained by the fact that the performance of the reduced-complexity DR improves under three-symbol observation window due to better approximation and less approximation errors. However, since the reduced-complexity HR approximates only the strong eigenvalues, it remains robust to ISI under both one-symbol and three-symbol observation window.

In the next experiment, we compare the performance of all receivers of interest namely, DR, CR, HR, reduced-complexity DR, reduced-complexity HR, average MMSE receiver, reduced-complexity MMSE receiver, and max-SINR receiver. For the average MMSE receiver and the reduced-complexity MMSE receiver, we consider two different scenarios: 1) the receiver has perfect knowledge of $\bar{\mathbf{R}}$ and the channel from the serving base station to the desired mobile and 2) the receiver has estimated information of $\bar{\mathbf{R}}$ and the channel from the serving base station

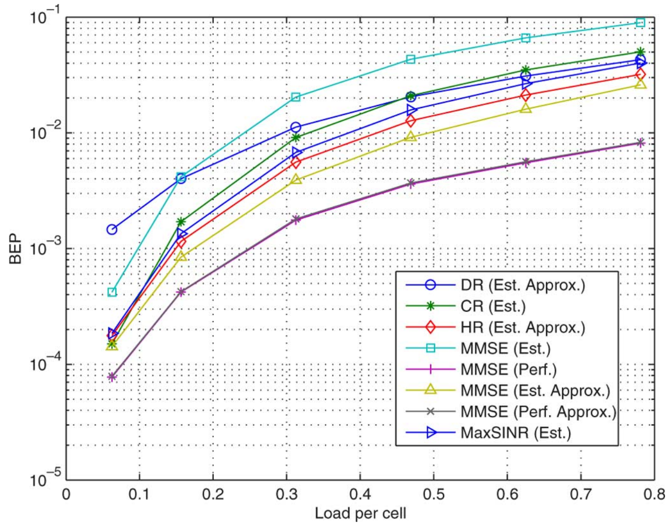

Fig. 7. BEP as a function of load per cell for six fades within the frame using both perfect and estimated CSI.

to the desired mobile. Since our focus is on designing low-complexity receivers, we employ a matched filter receiver to estimate multipath channel coefficients. In this experiment, a frame of a user consists of 96 gray encoded QPSK symbols and its duration is 20 ms. For velocity $v = 45$ mi/hour and carrier frequency $f_c = 2$ GHz, the number of fades per path over one frame is approximately 6. Here SNR $= 15$ dB per dimension and $L = 2$. In Fig. 7, we plot the performance (BEP) of these receivers as a function of the load per cell. Notice the difference in performance of MMSE (Perf.) and MMSE (Est.) in Fig. 7. At a target BEP $= 10^{-2}$, MMSE (Est.) suffers from a 71% decrease in capacity from the capacity of MMSE (Perf.). This result agrees with our discussion in Section III-F. Fig. 7 also shows that at a target BEP $= 10^{-2}$, with HR (Est. Approx.), the capacity increases almost by 72%, 48%, 30%, and 10% over the capacity with MMSE (Est.), DR (Est. Approx.), CR (Est.), and MaxSINR (Est.), respectively. The proposed MMSE (Est. Approx.) performs better than HR (Est. Approx.) at a price of at least ten times higher complexity.

V. Conclusion

In this paper, we propose a novel low-complexity hybrid receiver (HR) for the downlink of a multipath multicell CDMA system with TDD transmission scheme. The proposed receiver HR provides a tradeoff between the interference suffered by CR and the enhanced intercell interference and Gaussian noise suffered by DR. In addition, HR preserves the key advantageous feature of CR and DR, namely that it operates without the knowledge of other users' spreading codes. Using the circulant approximation of the channel autocorrelation matrix and the average received correlation matrix, we derive reduced-complexity HR and DR, and reduced-complexity MMSE receiver, respectively. Both the reduced-complexity HR and reduced-complexity MMSE receiver provide considerable capacity gain over CR. The reduced-complexity MMSE receiver performs slightly better than reduced-complexity HR at a price of higher complexity.

Appendix

Proof of Theorem 1: To prove Theorem 1, we assume that all orthogonal codes in the desired cell are in use, thus $K = N$. When user 1 wants to decode all in-cell users' symbols by using DR, from (6), we can write the DR for all K users as

$$\mathbf{\Phi}_{\mathrm{DR}}^{\dagger} = \mathbf{S}^{\dagger}(\mathbf{H}^{\dagger}\mathbf{H})^{-1} \tag{21}$$

where $\mathbf{S}$ is an $N \times N$ matrix whose columns are the orthonormal codes of all users. If user 1 wants to decode the symbols of all in-cell users by using the conventional decorrelating receiver of [12], it will first apply the matched filtering operation to the MRC output and then apply the inverse of the autocorrelation matrix. Therefore, the entire filtering operation used by the decorrelating receiver [12] is $\mathbf{\Phi}_{\mathrm{DEC}}^{\dagger} = \mathbf{\Gamma}^{-1}\mathbf{S}^{\dagger}$, where $\mathbf{\Gamma} = \mathbf{S}^{\dagger}\mathbf{H}^{\dagger}\mathbf{H}\mathbf{S}$ is the cross-correlation matrix of the in-cell received spreading sequences. Since the codes are orthonormal, $\mathbf{S}^{\dagger} = \mathbf{S}^{-1}$, which allows us to write $\mathbf{\Gamma}^{-1} = \mathbf{S}^{\dagger}(\mathbf{H}^{\dagger}\mathbf{H})^{-1}\mathbf{S}$ and

$$\mathbf{\Phi}_{\mathrm{DEC}}^{\dagger} = \mathbf{S}^{\dagger}(\mathbf{H}^{\dagger}\mathbf{H})^{-1}\mathbf{S}\mathbf{S}^{-1} = \mathbf{S}^{\dagger}(\mathbf{H}^{\dagger}\mathbf{H})^{-1}. \tag{22}$$

Comparing (22) with (21), we obtain the desired result.

Derivation of $\mathbb{E}_{\mathrm{CR}}$*,* I_{CR} *and* σ_{CR}^2*:* Note that $\mathbf{H}^{\dagger}\mathbf{H}$ is a Hermitian matrix. Thus, $y_{\mathrm{CR}}^{(\mathrm{d})} = \sqrt{P_1}\mathbf{s}_1^{\dagger}\mathbf{H}^{\dagger}\mathbf{H}\mathbf{s}_1$ is real. Since EVD of $\mathbf{H}^{\dagger}\mathbf{H}$ yields $\mathbf{H}^{\dagger}\mathbf{H} = \sum_{j=1}^{N}\lambda_j\mathbf{u}_j\mathbf{u}_j^{\dagger}$ squaring $y_{\mathrm{CR}}^{(\mathrm{d})}$ first and then using EVD of $\mathbf{H}^{\dagger}\mathbf{H}$, we obtain the instantaneous power of symbol b_1 at the output of CR as

$$\mathbb{E}_{\mathrm{CR}} = P_1\left(\sum_{j=1}^{N}\lambda_j\left|\mathbf{s}_1^{\dagger}\mathbf{u}_j\right|^2\right)^2. \tag{23}$$

Next, we derive the average power of the intracell interference for symbol b_1 at the output of CR. Squaring the magnitude of $y_{\mathrm{CR}}^{(\mathrm{i})}$, we obtain $|\, y_{\mathrm{CR}}^{(\mathrm{i})}\,|^2 = \sum_{q=2}^{K}\sum_{q'=2}^{K}\sqrt{P_q}\sqrt{P_{q'}}b_q b_{q'}\mathbf{s}_1^{\dagger}\mathbf{H}^{\dagger}\mathbf{H}\mathbf{s}_q\mathbf{s}_{q'}^{\dagger}\mathbf{H}^{\dagger}\mathbf{H}\mathbf{s}_1$. Since the information symbols of different users are independent with zero-mean and $|\, b_q\,|^2 = 1$, taking expectations of both sides of the above expression with respect to information symbols first and then using the EVD of $\mathbf{H}^{\dagger}\mathbf{H}$, we obtain the average intracell interference power as

$$I_{\mathrm{CR}} = \sum_{q=2}^{K}P_q\left|\sum_{j=1}^{N}\lambda_j\mathbf{s}_1^{\dagger}\mathbf{u}_j\mathbf{u}_j^{\dagger}\mathbf{s}_q\right|^2. \tag{24}$$

Squaring the magnitudes of n_{CR} of (4), then taking expectations with respect to Gaussian noise and applying EVD of $\mathbf{H}^{\dagger}\mathbf{H}$, we obtain the average noise power at the output of CR as

$$\sigma_{\mathrm{CR}}^2 = \sigma^2\sum_{j=1}^{N}\lambda_j\left|\mathbf{s}_1^{\dagger}\mathbf{u}_j\right|^2. \tag{25}$$

Derivation of $y_{\mathrm{HR}}^{(d)}$ *and* $y_{\mathrm{HR}}^{(i)}$*:* The desired part in the HR output is

$$y_{\mathrm{HR}}^{(\mathrm{d})} = \left(\sum_{j=1}^{M}\frac{1}{\lambda_j}\mathbf{s}_1^{\dagger}\mathbf{u}_j\mathbf{u}_j^{\dagger} + \sum_{j=M+1}^{N}\mathbf{s}_1^{\dagger}\mathbf{u}_j\mathbf{u}_j^{\dagger}\right)\sqrt{P}_1 b_1\mathbf{H}^{\dagger}\mathbf{H}\mathbf{s}_1.$$

Applying EVD of $\mathbf{H}^\dagger\mathbf{H}$ to the above equation first and then using the fact that the eigenvectors of $\mathbf{H}^\dagger\mathbf{H}$ are orthonormal, we obtain $y_{\mathrm{HR}}^{(\mathrm{d})}$ as

$$\sqrt{P}_1 b_1 \left(\sum_{j=1}^{M}\left|\mathbf{s}_1^\dagger\mathbf{u}_j\right|^2 + \sum_{j=M+1}^{N}\lambda_j\left|\mathbf{s}_1^\dagger\mathbf{u}_j\right|^2\right). \quad (26)$$

Similarly, we obtain $y_{\mathrm{HR}}^{(\mathrm{i})}$ as

$$\sum_{q=2}^{K}\sqrt{P}_q b_q \left(\sum_{j=1}^{M}\mathbf{s}_1^\dagger\mathbf{u}_j\mathbf{u}_j^\dagger\mathbf{s}_q + \sum_{j=M+1}^{N}\lambda_j\mathbf{s}_1^\dagger\mathbf{u}_j\mathbf{u}_j^\dagger\mathbf{s}_q\right). \quad (27)$$

Derivation of $\mathbb{E}_{\mathrm{HR}}$, I_{HR}, *and* σ_{HR}^2*:* Squaring the magnitude of $y_{\mathrm{HR}}^{(\mathrm{d})}$ in (26), we obtain the instantaneous power at the output of HR as

$$\mathbb{E}_{\mathrm{HR}} = P_1\left(\sum_{j=1}^{M}\left|\mathbf{s}_1^\dagger\mathbf{u}_j\right|^2 + \sum_{j=M+1}^{N}\lambda_j\left|\mathbf{s}_1^\dagger\mathbf{u}_j\right|^2\right)^2. \quad (28)$$

Squaring the magnitude of $y_{\mathrm{HR}}^{(\mathrm{i})}$ in (27), then taking expectation with respect to information symbols and using the fact that information symbols of different users are independent with zero-mean and $|b_q|^2 = 1$, we obtain the average intracell interference power at the output of HR as

$$I_{\mathrm{HR}} = \sum_{q=2}^{K}P_q\left|\sum_{j=1}^{M}\mathbf{s}_1^\dagger\mathbf{u}_j\mathbf{u}_j^\dagger\mathbf{s}_q + \sum_{j=M+1}^{N}\lambda_j\mathbf{s}_1^\dagger\mathbf{u}_j\mathbf{u}_j^\dagger\mathbf{s}_q\right|^2. \quad (29)$$

Squaring both sides of (14) and taking expectation with respect to Gaussian noise, we obtain

$$\begin{aligned}\sigma_{\mathrm{HR}}^2 &= \sigma^2\sum_{j=1}^{M}\frac{1}{\lambda_j}\mathbf{s}_1^\dagger\mathbf{u}_j\mathbf{u}_j^\dagger\mathbf{H}^\dagger\mathbf{H}\sum_{k=1}^{M}\frac{1}{\lambda_k}\mathbf{u}_k\mathbf{u}_k^\dagger\mathbf{s}_1\\ &\quad+\sigma^2\sum_{j=M+1}^{N}\mathbf{s}_1^\dagger\mathbf{u}_j\mathbf{u}_j^\dagger\mathbf{H}^\dagger\mathbf{H}\sum_{k=1}^{M}\frac{1}{\lambda_k}\mathbf{u}_k\mathbf{u}_k^\dagger\mathbf{s}_1\\ &\quad+\sigma^2\sum_{j=1}^{M}\frac{1}{\lambda_j}\mathbf{s}_1^\dagger\mathbf{u}_j\mathbf{u}_j^\dagger\mathbf{H}^\dagger\mathbf{H}\sum_{k=M+1}^{N}\mathbf{u}_k\mathbf{u}_k^\dagger\mathbf{s}_1\\ &\quad+\sigma^2\sum_{j=M+1}^{N}\mathbf{s}_1^\dagger\mathbf{u}_j\mathbf{u}_j^\dagger\mathbf{H}^\dagger\mathbf{H}\sum_{k=M+1}^{N}\mathbf{u}_k\mathbf{u}_k^\dagger\mathbf{s}_1.\end{aligned}$$

Applying EVD of $\mathbf{H}^\dagger\mathbf{H}$ along with the fact that the eigenvectors of $\mathbf{H}^\dagger\mathbf{H}$ are orthonormal to the above equation, we get

$$\sigma_{\mathrm{HR}}^2 = \sigma^2\left(\sum_{j=1}^{M}\frac{1}{\lambda_j}\left|\mathbf{s}_1^\dagger\mathbf{u}_j\right|^2 + \sum_{j=M+1}^{N}\lambda_j\left|\mathbf{s}_1^\dagger\mathbf{u}_j\right|^2\right). \quad (30)$$

REFERENCES

[1] C. D. Frank and E. Visotsky, "Adaptive interference suppression for direct-sequence CDMA systems with long spreading codes," in *Proc. IEEE 36th Annu. Allerton Conf. Communication, Control Computing*, Monticello, IL, Sep. 1998.

[2] S. Werner and J. Lilleberg, "Downlink channel decorrelation in CDMA systems with long codes," in *Proc. IEEE Int. Vehicular Technology Conf. (VTC)*, Houston, TX, May 1999, pp. 1614–1617.

[3] S. Chowdhury, M. D. Zoltowski, and J. S. Goldstein, "Reduced-rank chip-level MMSE equalization for the 3 G CDMA forward link with code-multiplexed pilot," *EURASIP J. Appl. Signal Process.*, vol. 2002, pp. 771–786, Aug. 2002.

[4] I. D. Ghauri and T. M. Slock, "Linear receivers for the CDMA Downlink Exploiting Orthogonality of spreading sequences," in *Proc. 32nd Asilomar Conf. Signals, Systems, Computers*, Asilomar, CA, Nov. 1998, pp. 650–654.

[5] K. Rohani and L. Jalloul, "Orthogonal transmit diversity for direct spread CDMA," in *Proc. Eur. Telecommunication Standard Institute Special Mobile Group 2*, Stockholm, Sweden, Sep. 1997.

[6] S. M. Alamouti, "A simple transmit diversity technique for wireless communications," *IEEE Trans. Commun.*, vol. 8, pp. 1451–1458, Oct. 1998.

[7] B. Hochwald, T. L. Marzetta, and C. B. Papadias, "A transmitter diversity scheme for wideband CDMA systems based on space-time spreading," *IEEE J. Sel. Areas Commun.*, vol. 19, pp. 48–60, Jan. 2001.

[8] A. Wittneben, "A new bandwidth efficient transmit antenna modulation diversity scheme for linear digital modulation," in *Proc. IEEE Int. Conf. Communications (ICC)*, Atlanta, GA, May 1993, pp. 1630–1634.

[9] D. Rajan, E. Erkip, and B. Aazhang, "Spreading and power allocation for multiple antenna transmission using decorrelating receivers," *IEEE Trans. Wireless Commun.*, vol. 2, pp. 436–445, May 2003.

[10] C. D. Frank, "MMSE reception of DS-CDMA with open-loop transmit diversity," in *Proc. 2nd Int. Conf. 3G Mobile Communications Technologies (IEE)*, London, U.K., Mar. 2001.

[11] M. Lenardi, A. Medles, and T. M. Slock, "Comparison of downlink transmit diversity schemes for RAKE and SINR maximizing receivers," in *Proc. IEEE Int. Conf. Communications (ICC)*, Helsinki, Finland, Jun. 2001, vol. 6, pp. 1679–1683.

[12] S. Verdú, *Multiuser Detection*. Cambridge, U.K.: Cambridge Univ. Press, 1998.

[13] R. Lupas and S. Verdú, "Linear multiuser detectors for synchronous code-division multiple-access channels," *IEEE Trans. Inf. Theory*, vol. 35, pp. 123–136, Jan. 1989.

[14] ——, "Near-far resistance of multiuser detectors in asynchronous channels," *IEEE Trans. Commun.*, vol. 38, pp. 496–508, Apr. 1990.

[15] Z. Xie, R. T. Short, and C. K. Rushforth, "A family of sub-optimum detectors for coherent multiuser communications," *IEEE J. Sel. Areas Commun.*, vol. 8, no. 4, pp. 683–690, Mar. 1990.

[16] U. Madhow and M. L. Honig, "MMSE interference suppression for direct-sequence spread-spectrum CDMA," *IEEE Trans. Commun.*, vol. 42, no. 12, pp. 3178–3188, Dec. 1994.

[17] M. Saquib and R. Yates, "Analysis of a partial decorrelator in a multi-cell DS/CDMA system," *IEEE Trans. Commun.*, Dec. 2002.

[18] R. M. Gray, *Toeplitz and Circulant Matrices: A Review*. Stanford, CA: Stanford University, 2002 [Online]. Available: http://ee.stanford.edu/~gray/toeplitz.pdf

[19] G. Strang, *Linear Algebra and its Applications*. Orlando, FL: Harcourt, 1988.

[20] T. S. Rappaport, *Wireless Communications Principles and Practice*. Upper Saddle River, NJ: Prentice-Hall, 1996.

Md Habibul Islam received the M.Sc. degree in electrical engineering from Tajik Technical University, Tajikistan, in 1995, the M.B.A. degree in finance from the Institute of Business Administration (IBA), the University of Dhaka, Bangladesh, in 1999, and the M.S. degree in electrical engineering and the Ph.D. degree in and telecommunications engineering from the University of Texas at Dallas in 2002 and 2005, respectively. His dissertation focused on the interference suppression schemes for the downlink of multiple-antenna code-division multiple-access (CDMA) systems.

In February 2006, he joined the Institute for Infocom Research (I2R), Singapore, as a Research Fellow, where he is working on the multiple-antenna schemes for IEEE 802.22 Wireless Regional Area Networks (WRAN) standard. His research interests include cognitive radio, orthogonal frequency-division multiplexing/orthogonal frequency-division multiple-access (OFDM/OFDMA), and multiple-antenna technology, such as space–time coding and beamforming.

Mohammad Saquib (M'98) received the B.Sc. degree in electrical and electronics engineering from Bangladesh University of Engineering & Technology, Bangladesh, in 1991 and the M.S. and Ph.D. degrees, both in electrical engineering, from Rutgers University, New Brunswick, NJ, in 1995 and 1998, respectively.

After his baccalaureate, from 1991 to 1992, he worked as a System Analyst at the Energy Research Corporation, Danbury, CT. During his graduate studies, he was a Graduate Research Assistant in the Wireless Information Networks Laboratory (WINLAB), Rutgers University. From 1998 to 1999, he was with the MIT Lincoln Laboratory, Lexington, MA, as a Member of the Technical Staff. In January 1999, he joined the Electrical and Computer Engineering Department at Louisiana State University, Baton Rouge, where he was the Donald Ceil & Elaine T. Delaune Endowed Assistant Professor. Since July 2000, he has been with the Electrical Engineering Department at the University of Texas at Dallas, where presently he is an Associate Professor. His research interests include various aspects of wireless data transmission, including system modeling and performance, signal processing and radio resource management, with emphasis on open-access techniques for spectrum sharing.

Prof. Saquib is an Associate Editor of the IEEE COMMUNICATIONS LETTERS and the IEEE TRANSACTIONS ON WIRELESS COMMUNICATIONS. He received the Best Teaching Award "for excellence in teaching Electrical Engineering and Telecommunications Classes," from the Dean of the School of Engineering, the University of Texas at Dallas for 2002–2003.

Naofal Al-Dhahir (M'90–SM'98) received the M.S. and Ph.D. degrees, both in electrical engineering, from Stanford University, Stanford, CA, in 1990 and 1994, respectively.

He was an Instructor at Stanford University in 1993. From August 1994 to July 1999, he was a Member of the Technical Staff at GE R&D Center, New York, where he worked on various aspects of satellite communication systems design and antijam GPS receivers. From August 1999 to July 2003, he was a Principal Member of Technical Staff at AT&T Shannon Laboratory, Florham Park, NJ, where he worked on space–time coding and signal processing. Currently, he is an Associate Professor at the University of Texas at Dallas. He has authored over 145 journal and conference papers and holds 16 U.S. patents. He is coauthor of the book *Doppler Applications for LEO Satellite Systems* (New York: Springer, 2002). His current research interests include space–time coding and signal processing, orthogonal frequency-division multiplexing (OFDM), wireless networks, and digital subscriber line technology.

Dr. Al-Dhahir is a member of the IEEE SP4COM and SPTM technical committees. He served as Editor for the IEEE TRANSACTIONS ON SIGNAL PROCESSING and the IEEE COMMUNICATIONS LETTERS and is currently an Editor for the IEEE TRANSACTIONS ON COMMUNICATIONS. He served as Co-Chair of the Communication Theory Symposium at the IEEE Global Telecommunications Conference (IEEE GLOBECOM) 2004. He received the Best Paper Award at the IEEE Vehicular Technology Conference (VTC) Fall 2005 conference and is corecipient of the 2005 IEEE Signal Processing Society Young Author Best Paper Award and the 2006 IEEE Donald G. Fink Best Paper Award.